Inorg. Chem. **2006**, *45*, 2903–2916

Electronic Properties, Redox Behavior, and Interactions with H_2O_2 of pH-Sensitive Hydroxyphenyl-1,2,4-triazole-Based Oxovanadium(V) Complexes

Wesley R. Browne,[†] Alette G. J. Ligtenbarg,[†] Johannes W. de Boer,[†] Tieme A. van den Berg,[†] Martin Lutz,[‡] Anthony L. Spek,[‡] František Hartl,[§] Ronald Hage,*[,||] and Ben L. Feringa*[,†]

Department of Organic and Molecular Inorganic Chemistry, Stratingh Institute, University of Groningen, Nijenborgh 4, 9747 AG Groningen, The Netherlands, Bijvoet Center for Biomolecular Research, Crystal and Structural Chemistry, Utrecht University, Padualaan 8, 3584 CH Utrecht, The Netherlands, van't Hoff Institute for Molecular Sciences, University of Amsterdam, Nieuwe Achtergracht 166, 1018 WV Amsterdam, The Netherlands, and Unilever R&D, Oliver van Noortlaan 120, 3133 AT, Vlaardingen, The Netherlands

Received October 25, 2005

The syntheses and spectroscopic characterization of two 1,2,4-triazole-based oxovanadium(V) complexes are reported: **1**$^-$ $[VO_2L1]^-$ and **2** $[(VOL2)_2(OMe)_2]$ (where H_2L1 = 3-(2′-hydroxyphenyl)-5-(pyridin-2′′-yl)-1*H*-1,2,4-triazole, H_3L2 = bis-3,5-(2′-hydroxyphenyl)-1*H*-1,2,4-triazole). The ligand environment (N,N,O vs O,N,O) is found to have a profound influence on the properties and reactivity of the complexes formed. The presence of the triazolato ligand allows for pH tuning of the spectroscopic and electrochemical properties, as well as the interaction and stability of the complexes in the presence of hydrogen peroxide. The vanadium(IV) oxidation states were generated electrochemically and characterized by UV–vis and EPR spectroscopies. For **2**, under acidic conditions, rapid exchange of the methoxide ligands with solvent [in particular, in the vanadium(IV) redox state] was observed.

Introduction

In recent years, interest in the coordination[1] and catalytic[2] chemistry of vanadium has grown primarily because of the recognition of its role in enzymatic systems, in particular, the haloperoxidases[3] found in marine fungi and algae (e.g., *Rhodophyceae, Ascophyllum nodosum*)[4] and in mushrooms (e.g., *amavadin*),[5] and more recently because of the insulin mimetic activity of vanadium(V) complexes.[6] Vanadium(V) centers are strong Lewis acids because of their low radius-to-charge ratio and are therefore suitable for the activation of peroxidic reagents.[1] Accordingly, vanadium(V) complexes have been found to act as catalyst precursors in various oxidation reactions such as bromination;[7] epoxidation of alkenes and allylic alcohols;[8] oxidation of sulfides to sulfoxides and sulfones,[9] phenols,[10] catechols,[11] and α-hydroxy esters;[12] hydroxylation of alkanes;[13] and oxidation

* To whom correspondence should be addressed. E-mail: B.L.Feringa@rug.nl (B.L.F.), Ronald.Hage@unilever.com (R.H.).
† University of Groningen.
‡ Utrecht University.
§ University of Amsterdam.
|| Unilever R&D.

(1) (a) Crans, D. C.; Smee, J. J. In *Comprehensive Coordination Chemistry II*, Wedd, A. G., Ed.; Elsevier/Pergamon: Oxford, U.K., 2004; Vol. 4, Chapter 4. (b) Crans, D. C.; Smee, J. J.; Gaidamauskas, E.; Yang, L. *Chem. Rev.* **2004**, *104*, 849−902.
(2) (a) Butler, A.; Clague, M. J.; Meister, G. *Chem. Rev.* **1994**, *94*, 625−638. (b) Ligtenbarg, A. G. J.; Hage, R.; Feringa, B. L. *Coord. Chem. Rev.* **2003**, *237*, 89−101. (c) Hirao, T. *Chem. Rev.* **1997**, *97*, 2707−2724.
(3) Butler, A.; Walker, J. V. *Chem. Rev.* **1993**, *93*, 1937−1944.
(4) (a) Gribble, G. W. *Acc. Chem. Res.* **1998**, *31*, 141−152. (b) Martinez, J. S.; Caroll, G. L.; Tschirret-Guth, R. A.; Altenhoff, G.; Little, R. D.; Butler, A. *J. Am. Chem. Soc.* **2001**, *123*, 3289−3294. (c) Carter-Franklin, J. N.; Butler, A. *J. Am. Chem. Soc.* **2004**, *126*, 15060−15066. (c) Butler, A.; Carrano, C. J. *Coord. Chem. Rev.* **1991**, *109*, 61−105.
(5) (a) Bayer, E.; Kneifel, H. *Z. Naturforsch. B* **1972**, *27*, 207. (b) Smith, P. D.; Berry, R. E.; Harben, S. M.; Beddoes, R. L.; Helliwell, M.; Collison, D.; Garner, C. D. *J. Chem. Soc., Dalton Trans.* **1997**, 4509−4516.
(6) (a) Liboiron, B. D.; Thompson, K. H.; Hanson, G. R.; Lam, E.; Aebischer, N.; Orvig, C. *J. Am. Chem. Soc.* **2005**, *127*, 5104−5115. (b) Crans, D. C.; Yang, L.; Jakusch, T.; Kiss, T. *Inorg. Chem.* **2000**, *39*, 4409−4416. (c) Melchior, M.; Rettig, S. J.; Liboiron, B. D.; Thompson, K. H.; Yuen, V. G.; McNeill, J. H.; Orvig, C. *Inorg. Chem.* **2001**, *40*, 4686−4690. (d) Shaver, A.; Ng, J. B.; Hall, D. A.; Lum, B. S.; Posner, B. I. *Inorg. Chem.* **1993**, *32*, 3109−3113. (e) Thompson, K. H.; McNeill, J. H.; Orvig, C. *Chem. Rev.* **1999**, *99*, 2561−2572.
(7) Clague, M. J.; Keder, N. L.; Butler, A. *Inorg. Chem.* **1993**, *32*, 4754−4761.
(8) (a) Bühl, M.; Schurhammer, R.; Imhof, P. *J. Am. Chem. Soc.* **2004**, *126*, 3310−3320. (b) Ell, A. H.; Jonsson, S. Y.; Börje, A.; Adolfsson, H.; Bäckvall, J.-E. *Tetrahedron Lett.* **2001**, *42*, 2569−2571.

10.1021/ic051848x CCC: $33.50
Published on Web 03/04/2006

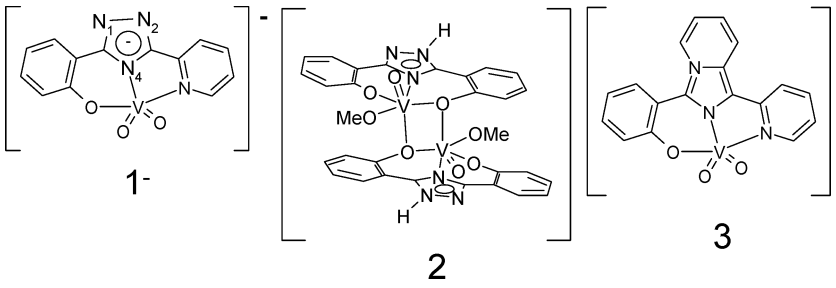

Figure 1. Structures of $\mathbf{1}^-$, **2**, and **3**.

of primary and secondary alcohols to their corresponding aldehydes and ketones.[2]

The majority of the known biologically relevant vanadium complexes, such as the vanadium haloperoxidases,[4] are coordinated by nitrogen- and oxygen-based donor ligands. However, within this coordination environment, there is considerable scope for variation, in terms of both ligand σ-donor and π-acceptor properties. Although phenol-,[14] salen-,[15] and pyridine carboxylate-[16] based ligands have received most attention for the formation of vanadium(IV) and vanadium(V) complexes, 1,2,4-triazole/phenolate-based ligands [e.g., H_2L1 = 3-(2′-hydroxyphenyl)-5-(pyridin-2″-yl)-1*H*-1,2,4-triazole, H_3L2 = bis-3,5-(2′-hydroxyphenyl)-1*H*-1,2,4-triazole; Figure 1] offer a new avenue in vanadium coordination chemistry, combining both the synthetic versatility of 1,2,4-triazoles and their well-established acid−base chemistry.[17] The triazole unit can coordinate to the metal ion in two ways: via N4 in an imidazole-type geometry (for the numbering pattern, see complex $\mathbf{1}^-$ in Figure 1) or via N1 in a pyrazole-type geometry. It can also act as a bridging unit between two metal centers, which involves metal coordination to N1 and N2 or more typically to N1 and N4.[18] Given the potential of this class of ligands, it is surprising that no examples of vanadium 1,2,4-triazole complexes have been reported to date. As part of our continuing investigation of the properties of vanadium(V) complexes, the synthesis and characterization of novel oxovanadium complexes based on triazole and phenolate ligands has been explored.[2b]

In the present contribution, the coordination chemistry of vanadium with 1,2,4-triazole-based ligands H_2L1 and H_3L2 (Figure 1) is examined, in the complexes $\mathbf{1}^-$ and **2**, respectively. The influence of ligand variation on the stability and reactivity of these vanadium complexes is studied by means of NMR, UV−vis, and EPR spectroscopies and spectroelectrochemistry. This study builds on our earlier investigation of the related dioxovanadium(V) complex (**3**) with the ligand 3-(2-hydroxyphenyl)-1-pyridin-2-yl-imidazo-[1,5-*a*]pyridine (Figure 1).[19] The pH-dependent interactions of complexes $\mathbf{1}^-$ and **2** with hydrogen peroxide and solvent are investigated, with particular emphasis on pH- and hydrogen peroxide-induced ligand labilization.

Experimental Section

Materials. All solvents employed were of HPLC grade and were used as received unless stated otherwise. All reagents employed in synthetic procedures were of reagent grade or better and were used as received. H_2L1[20] and H_3L2[21] (Figure 1) were synthesized by literature methods. H_2O_2 (50% w/w in H_2O) was obtained from Acros Organics.

$Na[VO_2L1]\cdot 2H_2O$ ($Na^+\mathbf{1}^-$). H_2L1 (80 mg, 0.34 mmol) and $NaVO_3$ (55 mg, 0.045 mmol, 1.3 equiv) were suspended in methanol (5 mL) and heated under reflux for 18 h. After the mixture had been cooled to room temperature, unreacted $NaVO_3$ and ligand were removed by filtration. The solution was evaporated to dryness

(9) (a) Bolm, C.; Bienewald, F. *Angew. Chem., Int. Ed. Engl.* **1995**, *34*, 2640−2641. (b) Sun, J.; Zhu, C.; Dai, Z.; Yang, M.; Pan, Y.; Hu, H. *J. Org. Chem.* **2004**, *69*, 8500−8503. (c) Blum, S. A.; Bergman, R. G.; Ellman, J. A. *J. Org. Chem.* **2003**, *68*, 150−155.
(10) Reis, P. M.; Silva, J. A. L.; Frausto da Silva, J. J. R.; Pombeiro, A. J. L. *J. Mol. Catal. A* **2004**, *224*, 189−195.
(11) (a) Yin, C.-X.; Finke, R. G. *J. Am. Chem. Soc.* **2005**, *127*, 9003−9013. (b) Battistel, E.; Tassinari, R.; Fornaroli, M.; Bonoldi, L. *J. Mol. Catal. A* **2003**, *202*, 107−115. (c) Yin, C.-X.; Finke, R. G. *J. Am. Chem. Soc.* **2005**, *127*, 13988−13996.
(12) Radosevich, A. T.; Musich, C.; Toste, F. D. *J. Am. Chem. Soc.* **2005**, *127*, 1090−1091.
(13) Cuervo, L. G.; Kozlov, Y. N.; Süss-Fink, G.; Shul'pin, G. B. *J. Mol. Catal. A: Chem.* **2004**, *218*, 171−177.
(14) (a) Redshaw, C.; Warford, L.; Dale, S. H.; Elsegood, M. R. J. *Chem. Commun.* **2004**, 1954−1955.
(15) (a) Balcells, D.; Maseras, F.; Ujaque, G. *J. Am. Chem. Soc.* **2005**, *127*, 3624−3634. (b) Ghosh, T.; Bhattacharya, S.; Das, A.; Mukherjee, G.; Drew, M. G. B. *Inorg. Chim. Acta* **2005**, *358*, 989−996. (c) Liu, Z.; Anson, F. C. *Inorg. Chem.* **2001**, *40*, 1329−1333. (d) Smith, K. I.; Borer, L. L.; Olmstead, M. M. *Inorg. Chem.* **2003**, *42*, 7410−7415. (e) Horn, A., Jr.; Filgueiras, C. A. L.; Wardell, J. L.; Herbst, M. H.; Vugman, N. V.; Santos, P. S.; Lopes, J. G. S.; Howie, R. A. *Inorg. Chim. Acta* **2004**, *357*, 4240−4246. (f) Pessoa, J. C.; Calhorda, M. J.; Cavaco, I.; Costa, P. J.; Correia, I.; Costa, D.; Vilas-Boas, L. F.; Felix, V.; Gillard, R. D.; Henriques, R. T.; Wiggins, R. *Dalton Trans.* **2004**, 2855−2866. (g) Ando, R.; Yagyu, T.; Maeda, M. *Inorg. Chim. Acta* **2004**, *357*, 2237−2244. (f) Root, C. A.; Hoeschele, J. D.; Cornman, C. R.; Kampf, J. W.; Pecoraro, V. L. *Inorg. Chem.* **1993**, *32*, 3855−3861. (g) Clague, M. J.; Keder, N. L.; Butler, A. *Inorg. Chem.* **1993**, *32*, 4754−4761.
(16) (a) Kimblin, C.; Bu, X.; Butler, A. *Inorg. Chem.* **2002**, *41*, 161−163. (b) Shul'pin, G. B.; Kozlov, Y. N.; Nizova, G. V.; Süss-Fink, G.; Stanislas, S.; Kitaygorodskiy, A.; Kulikova, V. S. *J. Chem. Soc., Perkin Trans. 2* **2001**, 1351−1371. (c) Crans, D. C.; Keramidas, A. D.; Amin, S. S.; Anderson, O. P.; Miller, S. M. *J. Chem. Soc., Dalton Trans.* **1997**, 2799−2812. (d) Mad'arova, M.; Sivak, M.; Kuchta, L.; Marek, J.; Benko, J. *Dalton Trans.* **2004**, 3313−3320. (e) Bonchio, M.; Conte, V.; Di Furia, F.; Modena, G.; Moro, S.; Edwards, J. O. *Inorg. Chem.* **1994**, *33*, 1631−1637. (f) Stover, J.; Rithner, C. D.; Inafuku, R. A.; Crans, D. C.; Levinger, N. E. *Langmuir* **2005**, *21*, 6250−6258.
(17) (a) Haasnoot, J. G. *Coord. Chem. Rev.* **2000**, *200*, 131−185. (b) Klingele, M. H. Brooker, S. *Coord. Chem. Rev.* **2003**, *241*, 119−132.
(18) Buchanan, B. E.; Wang, R.; Vos, J. G.; Hage, R.; Haasnoot, J. G.; Reedijk, J. *Inorg. Chem.* **1990**, *29*, 3263−3265.
(19) Ligtenbarg, A. G. J.; Spek, A. L.; Hage, R.; Feringa, B. L. *J. Chem. Soc., Dalton Trans.* **1999**, 659−661.
(20) Hage, R.; Haasnoot, J. G.; Reedijk, J.; Wang, R.; Ryan, E.; Vos, J. G.; Spek, A. L.; Duisenberg, A. J. M. *Inorg. Chim. Acta* **1990**, *174*, 77−85.
(21) (a) McConnan, J. *J. Chem. Soc., Trans.* **1907**, 196−199. (b) Ryabukhin, Y. I.; Faleeva, L. N.; Korobkova, V. G. *Chem. Heterocycl. Compd.* **1983**, *19*, 332−336.

and extracted with a minimum amount of methanol. Yellow needles of $Na^+\mathbf{1}^-$ (50 mg, 0.15 mmol, 44%) were obtained by infusion of diethyl ether. ^{1}H NMR (DMF-d_7): δ 9.02 (d, J = 5.1 Hz, 1H), 8.17 (dd, J = 7, 2 Hz, 1H), 8.12 (dt, J = 6, 1.5 Hz, 1H), 8.08 (dt, J = 8, 1.5 Hz, 1H), 7.48 (dd, J = 5.5, 1.2 Hz, 1H), 7.12 (dd, J = 6, 1 Hz, 1H), 6.75 (dt, J = 7, 1 Hz, 1H), 6.69 (t, J = 7 Hz, 1H). ESI-MS (CH_3OH): m/z 318.9 $[VO_2L1]^-$. Anal. Calcd for $C_{13}H_8N_4O_3V{\cdot}Na{\cdot}2H_2O$: C, 41.3; H, 3.19; N, 14.81%. Found: C, 42.6; H, 3.17; N, 14.63%.

$NH_4[VO_2L1]{\cdot}MeOH$ ($NH_4^+\mathbf{1}^-$). H_2L1 (80 mg, 0.34 mmol) and $NaVO_3$ (55 mg, 0.045 mmol, 1.3 equiv) were suspended in methanol (5 mL) and heated under reflux for 18 h. After the mixture had been cooled to room temperature, unreacted $NaVO_3$ was removed by filtration. NH_4PF_6 (219 mg, 1.34 mmol, 4 equiv) was added to the yellow solution. Yellow needles of $NH_4^+\mathbf{1}^-$ (50 mg, 0.15 mmol, 44%) were obtained by infusion of diethyl ether. ^{1}H NMR (DMF-d_7) δ 9.05 (d, J = 5.1 Hz, 1H), 8.22−8.12 (m, 2H), 8.09 (dd, J = 1.5, 7.7 Hz, 1H), 7.49 (dt, J = 1.8, 6.2 Hz, 1H), 7.12 (dt, J = 1.8, 7.9 Hz, 1H), 6.78 (d, 1H), 6.68 (t, 1H). ESI-MS (CH_3OH): m/z 318.9 $[VO_2L1^-]$. Anal. Calcd for $C_{13}H_8N_4O_3V{\cdot}NH_4\ CH_3OH$: C, 45.54; H, 4.37; N, 18.97%. Found: C, 45.21; H, 4.27; N, 18.84%. UV−vis (DMF): λ_{max} = 296 nm ($\epsilon_{max} = 4.3 \times 10^4$ M^{-1} cm^{-1}), 370 nm ($\epsilon_{max} = 1.6 \times 10^4$ M^{-1} cm^{-1}).

Crystal Structure Determination of $NH_4^+\mathbf{1}^-$. $NH_4[C_{13}H_8N_4O_3V]{\cdot}CH_3OH$, M_w = 369.26, yellow plate, 0.43 × 0.25 × 0.03 mm^3, triclinic, $P\bar{1}$ (No. 2), a = 8.7959(8) Å, b = 8.875(2) Å, c = 10.636(2) Å, α = 87.155(17)°, β = 72.165(14)°, γ = 79.154(14)°, V = 776.2(2) $Å^3$, Z = 2, D_x = 1.580 g cm^{-3}. An Enraf-Nonius CAD4T diffractometer with a rotating anode and graphite monochromator (λ = 0.71073 Å) was used to measure 5245 reflections up to a resolution of $(\sin\theta/\lambda)_{max}$ = 0.59 $Å^{-1}$ at T = 150(2) K. An absorption correction was applied (PLATON,[22] routine DELABS, μ = 0.67 mm^{-1}, 0.43−0.81 correction range). Of the measured reflections, 2738 were unique (R_{int} = 0.064). The structure was solved with automated Patterson methods[23] and refined with SHELXL-97[24] on F^2 of all reflections. Non-hydrogen atoms were refined with anisotropic displacement parameters. All hydrogen atoms were introduced in calculated positions. NH and OH hydrogen atoms were refined freely with isotropic displacement parameters; all other H atoms were refined as rigid groups. In all, 237 parameters were refined with no restraints. R1/wR2 [$I > 2\sigma(I)$] = 0.0519/0.0955. R1/wR^2 (all reflns) = 0.0976/0.1094. S = 1.026. Residual electron density between −0.38 and 0.32 e $Å^{-3}$. Geometry calculations, drawings, and checking for higher symmetry were performed with the PLATON package.[22]

$[(VOL2)_2(OCH_3)_2]{\cdot}2H_2O$ (2). H_3L2 (200 mg, 0.79 mmol) and $[VO(O^iPr)_3]$ (201 mg, 0.82 mmol, 1.04 equiv) were suspended in acetonitrile (10 mL) and stirred for 5 min. Methanol (10 mL) was added, and the solution stirred for 15 min whereupon the solution became clear. Dark green crystals of **2** were obtained by slow evaporation of the solvent (194 mg, 0.31 mmol, 77%). Crystals suitable for X-ray analysis were obtained after recrystallization from CH_3OH/CH_3CN. ^{1}H NMR [acetonitrile-d_3/DMSO-d_6 (1/1)]: δ 7.99 (d, J = 7.3 Hz, 2H), 7.39−7.34 (m, 2H), 6.95 (t, J = 7.3 Hz, 2H), 6.74 (d, J = 8.1 Hz, 2H). ESI-MS (CH_3OH): m/z 317.0 $[V^{IV}{}_2O_2(L2^{3-})_2]^{2-}$, m/z 634.9 $[(V^{IV}O(L2^{3-}))(V^{IV}O(HL2^{2-}))]^-$, m/z 652.0 $[((HL2^{2-})V^{IV}O)O(V^VO(L2^{3-}))]^-$, m/z 653.1 $[(V^{IV})_2O_2(HL2^{2-})_2(O)]^-$, m/z 666.0 $[((HL2^{2-})V^{IV}O)(OMe](V^VO(L2^{3-}))]^-$, m/z 667.1 $[H(V^{IV}O)_2(L2^{3-})_2(OMe)]^-$, m/z 347.9 $[V^VO(L2^{3-})(OMe)]^-$. Anal. Calcd for $C_{30}H_{24}N_6O_8V_2{\cdot}2H_2O$: C, 49.06; H, 3.84; N, 11.44%. Found: C, 49.33; H, 3.92; N, 11.46%. UV−vis (CH_3CN): λ_{max} = 309 nm ($\epsilon_{max} = 8.9 \times 10^3$ M^{-1} cm^{-1}), 390 nm ($\epsilon_{max} = 2.6 \times 10^3$ M^{-1} cm^{-1}).

Crystal Structure Determination of 2. $C_{30}H_{24}N_6O_8V_2{\cdot}2H_2O$, M_w = 734.46, red plate, 0.36 × 0.27 × 0.06 mm^3, monoclinic, Pc (No. 7), a = 8.0989(8) Å, b = 10.2358(16) Å, c = 18.537(3) Å, β = 90.557(10)°, V = 1536.7(4) $Å^3$, Z = 2, D_x = 1.587 g cm^{-3}. A Nonius KappaCCD diffractometer with a rotating anode and graphite monochromator (λ = 0.71073 Å) was used to measure 20666 reflections up to a resolution of $(\sin\theta/\lambda)_{max}$ = 0.59 $Å^{-1}$ at T = 150(2) K. An absorption correction was applied (PLATON,[22] routine DELABS, μ = 0.68 mm^{-1}, 0.53−0.85 correction range). Of the measured reflections, 5306 were unique (R_{int} = 0.053). The structure was solved with direct methods[25] and refined with SHELXL-97[24] on F^2 of all reflections. Non-hydrogen atoms were refined with anisotropic displacement parameters. All hydrogen atoms were located in the difference Fourier map. The hydrogen atoms of the water molecules were kept fixed in the located positions; all other H atoms were refined as rigid groups. In total, 436 parameters were refined with two restraints. R1/wR2 [$I > 2\sigma(I)$] = 0.0431/0.1027. R1/wR2 (all reflns) = 0.0551/0.1111. S = 1.150. Flack x parameter = 0.63(3). Residual electron density between −0.39 and 0.49 e $Å^{-3}$. Geometry calculations, drawings, and checking for higher symmetry were performed with the PLATON package.[22]

Instrumentation. ^{1}H NMR spectra (400.0 MHz) spectra were recorded on a Varian Mercury Plus spectrometer. Chemical shifts are denoted relative to the solvent residual peak (CHD_2CN, 1.94 ppm; CHD_2OD, 3.31 ppm). ^{51}V NMR spectra were recorded on a Varian Unity 500 spectrometer [131 MHz, relative to $\delta(VOCl_3)$ = 0 ppm]. Electrospray ionization mass spectra (ESI-MS) were recorded on a triple-quadrupole LC/MS/MS mass spectrometer (API 3000, Perkin-Elmer Sciex Instruments). Mass spectra were measured in positive and negative modes and in the range of m/z 100−1500. Conditions: ion-spray voltage = 5200 V, orifice = 15 V, ring = 150 V, Q0 = −10 V. UV−vis spectra were recorded on a diode-array Hewlett-Packard 8453 spectrophotometer. Elemental analyses were performed with a Foss-Heraeus CHN−O−Rapid or a EuroVector Euro EA elemental analyzer. FTIR spectra were recorded (as intimate mixtures in KBr) in reflectance mode, using a Nicolet Nexus FTIR spectrometer. Electrochemical measurements were carried out on a model 630B Electrochemical Workstation (CH Instruments). Analyte concentrations were typically 0.5−1 mM in anhydrous DMF, acetonitrile, or methanol containing 0.1 M tetrabutylammonium hexafluorophosphate (TBAP). Unless stated otherwise, a Teflon-shrouded glassy carbon working electrode (CH Instruments), a Pt wire auxiliary electrode, and a nonaqueous Ag/Ag^+ ion reference electrode were employed (calibrated externally using 0.1 mM solutions of ferrocene; all potentials reported are relative to SCE). Cyclic voltammograms were obtained at sweep rates between 10 and 100 mV s^{-1}. For reversible processes, the half-wave potential values are reported. Redox potentials were determined with a precision of ±10 mV. Bulk electrolysis experiments were performed in a homemade cell consisting of a 2-mm-path-length quartz cell, platinum gauze (Aldrich) working electrode, platinum wire counter electrode (separated from the bulk solution via a Vycor glass frit), and SCE reference electrode. EPR spectra

(22) Spek, A. L. *J. Appl. Crystallogr.* **2003**, *36*, 7−13.
(23) Beurskens, P. T.; Admiraal, G.; Beurskens, G.; Bosman, W. P.; Garcia-Granda, S.; Gould, R. O.; Smits, J. M. M.; Smykalla, C. *The DIRDIF99 Program System*; Technical Report of the Crystallography Laboratory; University of Nijmegen: Nijmegen, The Netherlands, 1999.
(24) Sheldrick, G. M. *SHELXL-97: Program for Crystal Structure Refinement*; Universität Göttingen, Göttingen, Germany, 1997.
(25) Sheldrick G. M. *SHELXS-97: Program for Crystal Structure Solution*; Universität Göttingen, Göttingen, Germany, 1997.

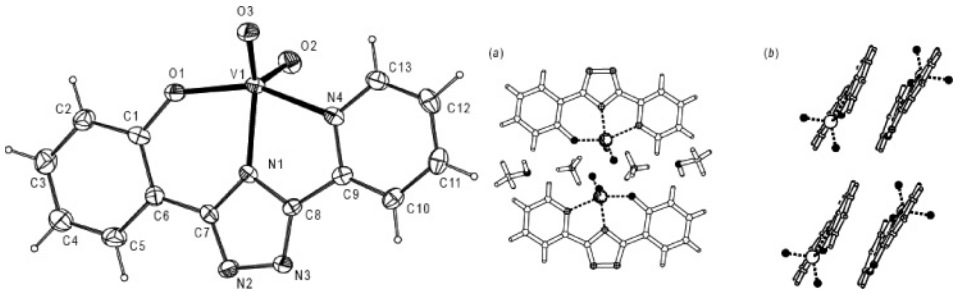

Figure 2. (Left) Displacement ellipsoid plot of $\mathbf{1}^-$ (50% probability). Ammonium ions and methanol solvent molecules have been omitted for clarity. (Right) Packing plots of $NH_4^+\mathbf{1}^-$ in the crystal.

(X-band) were recorded on a Bruker ECS106 instrument in liquid nitrogen (77 K). The preparation of samples for measurement by bulk electrolysis was monitored by UV−vis spectrometer prior to transfer of 0.25 mL of the electrolyzed solution to an EPR tube (frozen to 77 K immediately).

Results and Discussion

Syntheses and Structural Characterization. Triazole ligand H_2L1 was treated with sodium metavanadate ($NaVO_3$) in CH_3OH to yield the air-stable dioxovanadium(V) complex, which was isolated either directly as the sodium salt or as the NH_4^+ salt by crystallization from methanol/diethyl ether in the presence of an excess of NH_4PF_6. The formation of the complex was found to be dependent on the relative acidity of the solution. Addition of HPF_6 to the reaction (up to 2 equiv with respect to the ligand) resulted in the rapid formation of a yellow precipitate. Dissolution of the precipitate formed in DMF-d_7 occurred slowly but yielded a ^{1}H NMR spectrum (vide infra) identical to that of $\mathbf{1}^-$ obtained by heating at reflux under neutral conditions. From X-ray structural analysis (vide infra), it is apparent that the acid dependence of the rate and extent of the reaction of H_2L1 with sodium metavanadate is not due simply to protonation of the ligand. Indeed, given the high oxidation state of vanadium in the $[V^VO]^{3+}$ ion, deprotonation of the ligand ($L1^{2-}$) should favor complexation. Hence, the lack of complexation under more basic conditions can be ascribed to competition of methoxide and hydroxide ligands with H_2-L1. The rapid nature of the equilibrium between complexed and noncomplexed vanadium (in CH_3OH) is not unexpected given the absence of ligand field stabilization in the vanadium(V) oxidation state. The improved stability of $\mathbf{1}^-$ in the less firmly coordinating solvent DMF supports this hypothesis. Molecular plots and packing diagrams for $NH_4^+\mathbf{1}^-$ are shown in Figure 2. Selected bond distances and angles are collected in Table 1. The vanadium(V) ion is pentacoordinated by the pyridine nitrogen atom [2.170(3) Å], the phenolate oxygen [1.911(3) Å], a nitrogen of the triazole unit [2.031(3) Å], and two oxo groups [1.625(3) and 1.629(3) Å]. The triazole unit is deprotonated, and coordination to the vanadium occurs in an imidazole binding geometry (N1; see Figure 2 for crystallographic numbering scheme). The bond angle between the oxo groups at the vanadium center is 109.86(15)°. The triazole unit and the pyridine moiety of the ligand in $\mathbf{1}^-$ are almost planar [e.g., the torsion angle N4−C9−C8−N1 is 0.1(5)°]. However, the phenol unit is twisted compared to the nitrogen heterocycles [the torsion angle C1−C6−C7−N9 is −4.3(6)°], as shown in Figure 2. In the crystal lattice, one solvent molecule (CH_3OH) is incorporated per molecule of $NH_4^+\mathbf{1}^-$ accepting a hydrogen bond from the ammonium ion and donating a hydrogen bond to one of the V═O groups. The bond lengths and angles in $\mathbf{1}^-$ are similar to those observed in complex **3**,[19] as expected considering the very similar coordination environments of the two complexes. Nevertheless, some differences are observed because of the increased negative charge on the central heterocyclic ring (triazolato vs imidazole), in particular, the reduced V1−N1 distance [2.031(3) Å] in $\mathbf{1}^-$ compared to V1−N1 in **3** [2.090(3) Å].[19] Overall, however, the V−N and V−O bond lengths are comparable to those reported for related (ONN) vanadium(V) complexes.[26]

Table 1. Selected Bond Distances (Å) and Angles (deg) of Complex $NH_4^+\mathbf{1}^-$ with Standard Uncertainties in Parentheses

V−O1	1.911(3)	N2−N3	1.388(4)
V−O2	1.629(3)	N1−C8	1.349(5)
V−O3	1.624(3)	N3−C8	1.326(5)
V−N1	2.031(3)	N1−C7	1.364(5)
V−N4	2.170(3)	N2−C7	1.336(5)
O1−C1	1.355(4)		
O1−V−O2	104.70(13)	O3−V−N1	134.07(14)
O2−V−O3	109.86(15)	N1−V−N4	73.29(12)
O1−V−O3	99.00(13)	V−O1−C1	137.2(3)
O1−V−N4	153.06(12)	O2−V−N4	94.95(14)

The shortest intermolecular V···V distances in **1** and **3** are 6.2981(18) and 6.3508(18) Å, confirming the absence of direct or bridged V···V bonding interactions. For $\mathbf{1}^-$, negative-mode ESI-MS shows a parent ion at *m*/*z* 318.9, corresponding to $[VO_2L1]^-$. Under acidic conditions, no significant peaks assignable to vanadium(V) complexes were observed in either negative or positive mode, indicating that protonation, presumably at the 1,2,4-triazole moiety, yields a neutral complex ($[HVO_2L1]$).

In contrast to H_2L1, the dinuclear vanadium complex of H_3L2 (**2**) was obtained by reaction with $[VO(O^iPr)_3]$ in CH_3CN/CH_3OH (1/1 v/v). Dark green crystals suitable for X-ray analysis were obtained by slow evaporation of a CH_3OH/CH_3CN solution of the complex. For both **1** and **2**, it would

(26) (a) Hills, A.; Hughes, D. L.; Leigh, C. J.; Sanders, J. R. *J. Chem. Soc., Dalton Trans.* **1991**, 61−64. (b) Liu, H. X.; Wang, W.; Wang, X.; Tan, M. Y. *J. Coord. Chem.* **1994**, *33*, 347−352. (c) Giacomelli, A.; Floriani, C.; Ofir De Souza Duarte, A.; Chiesi-Villa, A.; Guastini, C. *Inorg. Chem.* **1982**, *21*, 3310−3316. (d) Root, C. A.; Hoeschele, J. D.; Cornman, C. R.; Kampf, J. W.; Pecoraro, V. L. *Inorg. Chem.* **1993**, *32*, 3855−3861. (e) Vergopoulos, V.; Priebsch, W.; Fritzche, M.; Rehder, D. *Inorg. Chem.* **1993**, *32*, 1844−1849.

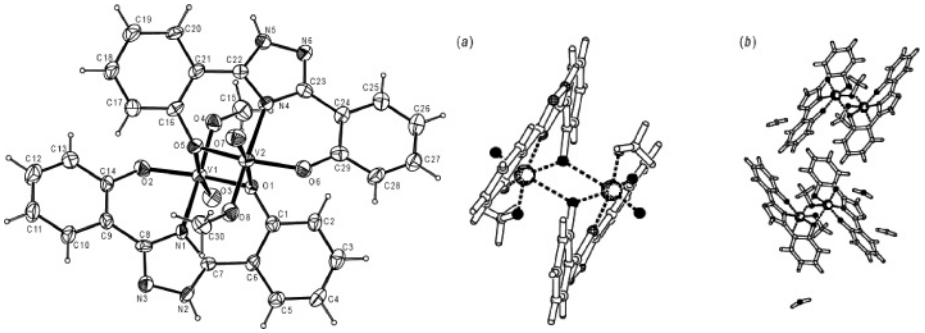

Figure 3. (Left) Displacement ellipsoid plot of **2** (50% probability). (Right) PLATON plots of **2**: (a) side view of the dinuclear complex and (b) spatial arrangement of **2** in the unit cell including H_2O molecules.

be anticipated that anionic ligands could favor complexation because of the high oxidation state of the vanadium center. However, the presence of oxo ligands increases electron density at the vanadium(V) centers, and as a result, weaker donor ligands bind more readily. An additional feature that is highlighted by the relative ease of coordination of ligands H_2L1 and H_3L2 to vanadium(V) is the importance of ligand bite angle,[27] with the ONO coordination of H_3L2 being more flexible, and hence more favorable, than the ONN coordination of H_2L1. In addition to ligand bite angle, the hard metal ion character of the VO_2^+ would be expected to favor coordination of hard ligands rather than good π-accepting ligands such as pyridine. Indeed, for the tridentate ligand 3,5-bis(pyidin-2′-yl)-1*H*-1,2,4-triazole, coordination to vanadium was not observed.[28] Complex **2** was isolated as a dinuclear complex (Figure 3), where each vanadium(V) ion is held in a partially distorted octahedral coordination environment, with two phenolic oxygens, the triazole nitrogen, and the methoxy group in the equatorial plane and an oxo group in one of the apical positions. The remaining (apical) position is occupied by a shared phenolic oxygen of the other ligand residue. In this manner, a V_2O_2 four-membered ring is formed with one phenolic oxygen of each ligand bridging between the two metal centers. Bond angles and lengths are reported in Table 2. The complex is approximately centrosymmetric, with V═O bond lengths of 1.594(4) Å for V1−O3 and 1.598(4) Å for V2−O7. These short distances are consistent with a strong trans influence[29] that is reflected in elongation of the V−O(phenolate) bonds trans to the oxo groups [V1−O5 is 2.352(4) Å and V2−O1 is 2.314(4) Å] (compared to the more common bond lengths for phenolato−V bonds of 1.85−2.01 Å).[26e,30] The intramolecular V···V distance is 3.4557(13) Å, suggesting that there is no direct interaction of the vanadium centers. The ligands

Table 2. Selected Bond Distances (Å), Angles (deg), and Torsion Angles (deg) of Complex **2** with Standard Uncertainties in Parentheses

V1−O1	1.945(3)	V2−O5	1.940(4)
V1−O2	1.856(4)	V2−O6	1.860(4)
V1−O3	1.594(4)	V2−O7	1.598(4)
V1−N1	2.108(4)	V2−O1	2.314(4)
V1−O5	2.352(4)	V2−N4	2.116(4)
N1−C8	1.349(7)	N4−C22	1.349(6)
N1−C7	1.365(6)	N4−C23	1.352(7)
N2−N3	1.369(6)	N5−N6	1.380(6)
O2−C14	1.364(7)	O5−C1	1.369(6)
O1−C1	1.375(6)	O6−C29	1.331(7)
O1−V1−O2	154.53(17)	O5−V2−O6	154.71(17)
O1−V1−N1	81.91(15)	O5−V2−N4	81.98(15)
O2−V1−N1	82.24(15)	O6−V2−N4	82.15(17)
V1−O1−V2	108.15(15)	V1−O5−V2	106.85(16)
O5−V1−O1−V2	1.64(15)	O3−V1−O4−C15	−22.2(5)

are oriented parallel to each other, but as with $\mathbf{1}^-$, they are not completely planar, with the bridging phenolate moiety showing a significant twist with respect to the triazole unit and the nonbridging phenolato unit. In contrast to $\mathbf{1}^-$, the triazole unit of **2** is not deprotonated. Overall, the coordination environment of **2** is similar to that of the complex bis-[2-(2′-hydroxyphenyl)-chinolin-8-olato]dimethoxo-dioxo-divanadium(V).[31] The strong preference of vanadium(V) for hexacoordination rather than pentacoordination[32] might be the driving force for the formation of a dinuclear complex in the solid state. Indeed, in related systems, mesityl,[33] aquo,[34] or oxo groups[35] serve as the bridging unit between the metal

(27) (a) Dani, P.; Karlen, T.; Gossage, R. A.; Gladiali, S.; Van Koten, G. *Angew. Chem., Int. Ed.* **2000**, *39*, 743−745. (b) Del Rio, J.; Back, S.; Hannu, M. S.; Rheinwald, G.; Lang, H.; Van Koten, G. *Inorg. Chim. Acta* **2000**, *300*, 1094−1098.

(28) No well-defined complexes could be obtained by reaction of 3,5-bis-(pyrid-2′-yl)-1*H*-1,2,4-triazole with (VO_2Cl_2[PPh_4]), $VO(O^iPr)_3$, $NaVO_3$, and NH_4VO_3 under an argon atmosphere in acetonitrile, diethyl ether, or methanol, and only starting materials were isolated after purification of the crude products, by ^{1}H NMR spectroscopic analysis and EI- and ESI-mass spectrometry.

(29) (a) Cornman, C. R.; Kampf, J.; Pecoraro, V. L. *Inorg. Chem.* **1992**, *31*, 1981−1983. (b) Kabanos, T. A.; Keramidas, A. D.; Papaioannou, A.; Terzis, A. *Inorg. Chem.* **1994**, *33*, 845−846. (c) Crans, D. C.; Shim, P. K. *Inorg. Chem.* **1988**, *27*, 1797−1806.

(30) (a) Hills, A.; Hughes, D. L.; Leigh, G. J.; Sanders, J. R. *J. Chem. Soc., Dalton Trans.* **1991**, 61−64. (b) Liu, H. X.; Wang, W.; Wang, X.; Tan, M. Y. *J. Coord. Chem.* **1994**, *33*, 347−352. (c) Giacomelli, A.; Floriani, C.; Ofir De Souza Duarte, A.; Chiesi-Villa, A.; Guastini, C. *Inorg. Chem.* **1982**, *21*, 3310−3316. (d) Root, C. A.; Hoeschele, J. D.; Cornman, C. R.; Kampf, J. W.; Pecoraro, V. L. *Inorg. Chem.* **1993**, *32*, 3855−3861.

(31) Hefele, H.; Uhlemann, E.; Weller, F.*Z. Naturforsch.* **1997**, *52b*, 693−695.

(32) (a) Oyaizu, K.; Yamamoto, K.; Yoneda, K.; Tsuchida, E. *Inorg. Chem.* **1996**, *35*, 6634−6635. (b) Asgedom, G.; Sreedhara, A.; Kivikoski, J.; Valkonen, J.; Kolehmainen, E.; Rao, C. P. *Inorg. Chem.* **1996**, *35*, 5674−5683.

(33) (a) Thiele, K.; Gorls, H.; Imhof, W.; Seidel, W. *Z. Anorg. Allg. Chem.* **2002**, *628*, 107−118. (b) Thiele, K.; Görls, H.; Imhof, W.; Seidel, W. *Z. Anorg. Allg. Chem.* **1999**, *625*, 1927−1933.

(34) Mimoun, H.; Chaumette, P.; Mignard, M.; Saussine, L. *Nouv. J. Chim.* **1983**, *7*, 467−475.

(35) (a) Mahroof-Tahir, M.; Keramidas, A. D.; Goldfarb, R. B.; Anderson, O. P.; Miller, M. M.; Crans, D. C. *Inorg. Chem.* **1997**, *36*, 1657−1668. (b) Duncan, C. A.; Copeland, E. P.; Kahwa, I. A.; Quick, A.; Williams, D. J. *J. Chem. Soc., Dalton Trans.* **1997**, 917−919. (c) Saneetha, N. R.; Pal., S. *Bull. Chem. Soc. Jpn.* **2000**, *73*, 357−363. (d) Plass, W.; Pohlmann, A.; Yozgatli, H.-P. *J. Inorg. Biochem.* **2000**, *80*, 181−183.

centers. However, binding modes similar to those observed in **2**, i.e., with a bridging phenolate moiety provided by the ligand, are less common in vanadium(V) complexes but are observed for vanadium(IV) species[1,36] such as the vanadium(IV) complex based on *N*,*N*-bis(2-hydroxybenzyl)aminoacetic acid.[37]

For **2**, the neutrality of the binuclear complex precludes the direct observation by ESI-MS of $[\{(HL2)V^{V}O(OCH_3)\}_2]$ or a mononuclear analogue in which the sixth coordination site is occupied by solvent. Nevertheless, in negative-mode ESI-MS, several ions are observed that could be assigned to corresponding monomeric and dimeric complexes with vanadium(IV) and vanadium(V) oxidation states and in the deprotonated state (see Experimental Section for details). The observation of vanadium(IV) species, under the MS conditions, is expected because of the quite accessible reduction potential of the complex (vide infra). The mass spectra of **2** were recorded in acetonitrile and in methanol. In the solid state, **2** exists as a neutral dinuclear complex with each metal center coordinated by $HL2^{2-}$, CH_3O^-, and O^{2-}. In solution, however, the dinuclear nature of the complex is not certain, and ligand deprotonation is possible. Moreover, the methoxide ligand is, potentially, susceptible to substitution by solvent. In methanol solution, negative ions corresponding to dinuclear complexes in the $V^{IV}V^{IV}$ and $V^{IV}V^{V}$ states (with loss of CH_3OH) as well as to mononuclear vanadium(V) species in which the ligand is deprotonated are observed. In acetonitrile, a much simpler negative-mode spectrum is obtained, with peaks observed at *m*/*z* 252 (H_2L2^-), 334, and 651. The peak at *m*/*z* 334 is assigned, tentatively, to the mononuclear complex $[V^{V}(HL2^{2-})O_2]^-$, and the peak at *m*/*z* 651 is assigned to $[\{V^{V}(L2^{3-})O\}_2OH]^-$. No evidence for acetonitrile coordination was obtained from the negative-ion mass spectra. However, replacement of the anionic methoxide ligand for acetonitrile would result in the formation of a neutral complex. Addition of HPF_6 resulted in reduced intensity of the peaks, with no new ions observed. In positive mode, no significant ions were observed either in the absence or in the presence of HPF_6.

FTIR spectra of $Na^+\mathbf{1}^-$, H_2L1, **2**, and H_3L2 were recorded in KBr powder (see Supporting Information, Figures S1 and S2). For H_2L1, complexation to the vanadium(V) center leads to a ~10 cm^{-1} blue shift of the phenolic ring breathing vibrations in the 1630−1600 cm^{-1} spectral region and the appearance of two new intense bands at 927 and 945 cm^{-1}, which are assigned to symmetric and asymmetric ν(O═V═O) vibrations, respectively.[2,16c,26] The ν(O═V═O) wavenumbers are in the range expected for dioxovanadium(V) compounds.[26] For H_3L2, complexation to vanadium(V) results in the appearance of a single strong ν(V═O) band at 874 cm^{-1} typical of hexacoordinate oxovanadium complexes.[16c,38] The medium-intensity absorption at 1035 cm^{-1} is indicative of the presence of a methoxide ligand.[39]

^{1}H and ^{51}V NMR Spectroscopy of 1^- and 2 in Neutral, Acidic, and Alkaline Media. The ^{1}H NMR spectrum of $\mathbf{1}^-$ was recorded in DMF-d_7 (see Supporting Information, Figure S3) and in methanol-d_4 under neutral, acidic, and basic conditions (Figure S4). In DMF-d_7, $\mathbf{1}^-$ is stable, and addition of base has no effect on the ^{1}H NMR spectrum. However, addition of HPF_6 induces a downfield shift of all resonances (Figure S5). In particular, the downfield shift of the H3 resonance of the pyridine ring (from 9.02 to 9.23 ppm) is similar to that observed for related complexes (e.g., $[Ru(bpy)_2(HL1)]^+$), suggesting protonation of the 1,2,4-triazolato ring (see Supporting Information, Figure S5).[18,40]

In contrast to DMF-d_7, in methanol-d_4, some free ligand is observed in the ^{1}H NMR spectrum. Addition of CH_3ONa results in complete ligand dissociation (Figure S4).[29] Under acidic conditions, the spectrum becomes more complex, with both protonation and, at very high HPF_6 concentrations, ligand dissociation also (Figures S4 and S6). Nevertheless, both direct addition of HPF_6 and addition of HPF_6 to a basic solution of $\mathbf{1}^-$ yield identical ^{1}H NMR spectra, indicating rapid complexation/decomplexation and availability of "free" vanadate under basic conditions. In each case, the expected eight resonances are observed for each species, and addition of base to acidic solutions (and vice versa) leads to rapid equilibration. Overall, the spectra of $\mathbf{1}^-$ observed in both methanol-d_4 and DMF-d_7 match closely, suggesting that the same species is present in both solvents. Surprisingly, in the presence of HPF_6, the ^{1}H NMR spectra of $\mathbf{1}^-$ recorded in methanol and DMF are very different. Two protonation steps can be discerned in methanol-d_4, leading to two separate sets of eight peaks each. Addition of 1 equiv of HPF_6 leads to protonation of $\mathbf{1}^-$, followed by rapid formation of a second species (Figure S6). Addition of excess HPF_6 (100 equiv) leads to ligand dissociation. The modest upfield shift of the H3 resonance (9.05 ppm) of the pyridyl ring in the second species formed indicates that, in methanol-d_4, protonation is followed by a change in the coordination environment from that observed in DMF (vide infra). ^{51}V NMR spectra of $\mathbf{1}^-$ were obtained in methanol-d_4 and in DMF-d_7. In DMF-d_7, a single absorption was observed at −450 ppm, and addition of HPF_6 (~0.5 equiv) resulted in the appearance of a new triplet absorption at −507 ppm (Figure S7).[41] This result, although unusual, is not unprecedented[42] and might indicate labilization of the pyridine moiety in acidic solution. This interpretation is supported by the fact that the overall breadth of the absorption at −450 ppm is similar to that of the triplet formed upon addition of HPF_6. Because the ^{14}N nucleus has a nuclear spin $I = 1$, a 1/1/1 pattern is observed upon coordination of nitrogen. For $\mathbf{1}^-$, two nitrogen atoms are coordinated, and hence, a multiplet is observed as a

(36) Syamal, A.; Kale, K. S. *Inorg. Chem.* **1979**, *18*, 992−995.

(37) Ceccato, A. S.; Neves, A.; De Brito, M. A.; Drechsel, S. M.; Mangrich, A. S.; Werner, R.; Haase, W.; Bortoluzzi, A. J. *J. Chem. Soc., Dalton Trans.* **2000**, 1573−1577.

(38) Micera, G.; Sanna, D. In *Vanadium in the Environment, Part One: Chemistry and Biochemistry*; Nriagu, J. O., Ed.; John Wiley & Sons: New York, 1998; Chapter 7.

(39) Syamal, A.; Theriot, L. J. *J. Coord. Chem.* **1973**, *2*, 193−200.

(40) Keyes, T. E.; Evrard, B.; Vos, J. G.; Brady, C.; McGarvey, J. J.; Jayaweera, P. *Dalton Trans.* **2004**, 2341−2346.

(41) Addition of one or more equivalents leads to a complete conversion to the protonated state.

(42) (a) Priebsch, W.; Rehder, D. *Inorg. Chem.* **1985**, *24*, 3058−3062. (b) Nugent, W. A.; Harlow, R. L. *J. Chem. Soc., Chem. Commun.* **1979**, 342−343.

broadened peak. The increased intensity of the central absorption of $\mathbf{1}^-$ in the presence of HPF_6, is assigned to relaxation decoupling[43] between the quadrupolar ^{14}N and ^{51}V nuclei. In methanol-d_4, a more complex acid−base behavior is observed (Figure S6), with two signals present at −471 (broad absorption) and −464 ppm (sharp singlet). Addition of 1 equiv of HPF_6 to $\mathbf{1}^-$ in methanol-d_4 leads to the formation of three broad peaks at −457, −485, and −512 ppm (very weak); however, within 1 h, the absorption at −485 ppm becomes the major species observed. Addition of 2 equiv of HPF_6 yields the same absorption at −485 ppm immediately. Addition of CH_3ONa to $\mathbf{1}^-$ in methanol-d_4 results in the disappearance of the −471 ppm absorption and increased intensity of the −464 ppm absorption. The sharp absorption is assigned to the vanadate ion liberated upon decomplexation of HL1 (by comparison with $NaVO_3$, Figures S8 and S9). Subsequent addition of HPF_6 leads to the appearance of a broad signal at −380 ppm identical to the signal observed upon addition of HPF_6 to $\mathbf{1}^-$ in methanol-d_4, i.e., protonated free vanadate (Figure S8). A second broad absorption is observed at −485 ppm, its intensity being dependent on the number of HPF_6 equivalents added (Figure S6, with excess HPF_6 it is not observed, vide supra).[44] The observation of two signals in the ^{51}V NMR spectrum arising from vanadium(V) complexed to L1 is in good agreement with the corresponding ^1H NMR spectrum, which shows two different sets of $L1^{2-}$ signals (neither set being assignable to free ligand) under the same conditions (Figure S6). It should be noted that the observation of free vanadate in the ^{51}V NMR spectrum of $\mathbf{1}^-$ in methanol and its absence in the spectrum obtained in DMF-d_7 corresponds with the presence and absence, respectively, of free H_2L1 in the ^1H NMR spectra. The similarity of the ^{51}V NMR spectra in methanol-d_4 and DMF-d_7 in the absence of HPF_6 is in stark contrast to the shift in the ^{51}V NMR spectra observed in the presence of HPF_6 (vide supra). In the presence of HPF_6, a downfield shift of the ^{51}V signal by 14 ppm in methanol-d_4 is observed, in contrast to the upfield shift of 57 ppm observed in DMF-d_7, indicating a difference in the coordination environment in the two solvents upon protonation. The subsequent upfield shift of 28 ppm of the absorption in methanol to −485 ppm indicates that, eventually, similar changes in coordination environment take place in both solvents.

From the X-ray structure of **2**, eight resonances would be anticipated in the ^1H NMR spectrum due to the two nonequivalent phenol groups of $HL2^{2-}$. However, in DMF-d_7, a single set of four resonances is observed for **2** (Figure 4). The breadth of the signals, however, raises the possibility that an exchange equilibrium is occurring in solution (i.e., the nonbridging and bridging phenol units exchange roles), and hence, on the ^1H NMR time scale, a dinuclear complex might yield an average signal for the two nonequivalent phenol rings. This is not unexpected in view of the fact that

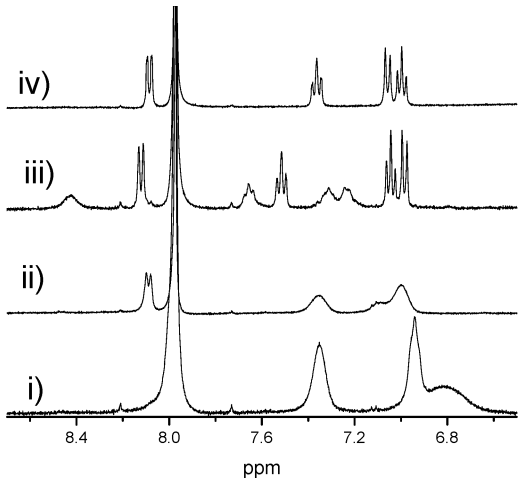

Figure 4. ^1H NMR (400 MHz) spectra of (i) **2**, (ii) **2** + H_2O_2, (iii) **2** with HPF_6, (iv) **2** with HPF_6 and then H_2O_2 (all spectra in DMF-d_7).

ligand exchange for $\mathbf{1}^-$ is very fast and reversible and the bridging phenoxide ligands of **2** have one normal and one extended V−O bond. Addition of HPF_6 leads to overall sharpening of the signals with a total of eight resonances observed, four of which are well-resolved and the remaining four of which show considerable broadening (Figure 4). Integration of each set of four resonances suggests that they do not arise from the same species; however, addition of several equivalents of HPF_6 does not result in further changes, excluding the involvement of two different protonation states. The increased difference in signal intensities after reaction with H_2O_2 (vide infra) supports the conclusion that each set of four signals corresponds to a distinct mononuclear (or at least a symmetric dinuclear) complex. In acetonitrile-d_3, the ^1H NMR spectrum of **2** (Figure S10) is less broadened than that in DMF-d_7. Again, only four aromatic resonances are observed, indicating that the two phenol rings of $HL2^{2-}$ are equivalent. However, addition of HPF_6 to **2** leads to a sharpening of the signals, with four resonances at chemical shifts similar to those observed in DMF-d_7. For both DMF-d_7 and acetonitrile-d_3, addition of base (CH_3ONa) had no observable effect on the ^1H NMR spectra.

In acetonitrile, the breadth of the ^1H NMR absorptions for **2** decreases with decreasing temperature, and at −15 °C in CD_3CN, several absorptions are observed, consistent with a mixture of mono- and dinuclear species in rapid equilibrium. In contrast, a reduction in the concentration of **2** leads to a significant sharpening of the absorption bands (Figure S10), but with only four signals observed. The absence of a significant temperature dependence in the ^{51}V NMR spectrum, which shows only a single absorption, indicates that, whereas **2** exists as a dimeric complex in the solid state, it is unlikely that a strong association of the two (HL2)V═O-(OCH_3) units persists in solution. In addition, the acid/base dependence of the spectra indicates that complex **2** deprotonates upon dissolution, which can be rationalized by a decrease in the pK_a of the 1,2,4-triazole group upon formation of the mononuclear pentacoordinate complex.[18]

(43) Minelli, M.; Hubbard, J. L.; Christensen, K. A.; Enemark, J. H. *Inorg. Chem.* **1983**, *22*, 2652−2653.

(44) The (reversible) dissociation of the ligand from the vanadium(V) center at low and high pH has been noted for related phenolate-based complexes; see: Jakusch, T.; Marcão, S.; Rodrigues, L.; Correia, I.; Pessoa, J. C.; Kiss, T. *Dalton Trans.* **2005**, 3072−3078.

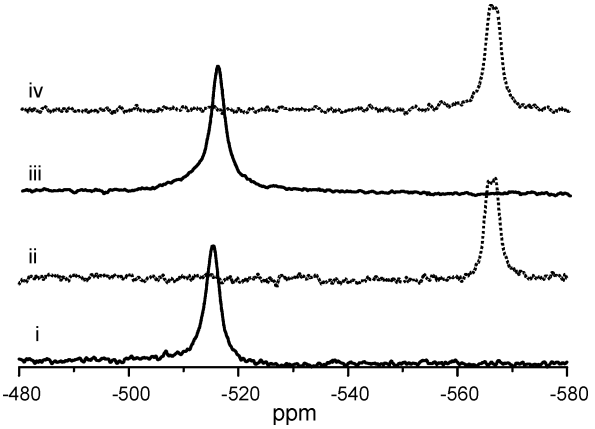

Figure 5. ^{51}V NMR spectra (131 MHz) of **2** in DMF-d_7 in the (i) absence and (ii) presence of HPF_6 and (iii, iv) 10 h after addition of H_2O_2.

In DMF-d_7, **2** gives a signal in the ^{51}V NMR spectrum at −515 ppm. Addition of HPF_6 leads to the appearance of a new signal at −565 ppm (doublet, Figure 5). In acetonitrile-d_3, a single resonance at −505 ppm is observed that shifts to −593.5 ppm (doublet) upon addition of HPF_6 (Figure S11). The difference in the chemical shifts observed for **2** in acetonitrile and DMF suggests that the coordination environment is modified, possibly through solvent coordination in the absence of HPF_6, and through ligand exchange of the methoxy unit under acidic conditions. The different UV−vis spectra obtained in acidified acetonitrile and DMF support this interpretation (vide infra).

Electronic Absorption Spectroscopy of 1^- and 2. The UV−vis spectrum of $\mathbf{1}^-$ in methanol shows a distinct pH dependence (Figure 6). In basic solution (CH_3ONa/CH_3OH), a very weak, broad absorption at ∼350 nm and two intense absorption bands at 245 and 286 nm are present. Addition of HPF_6 results in a decreased intensity of the 245 nm absorption band and in a bathochromic shift of both the 286 and ∼350 nm absorption bands to 305 and ∼380 nm, respectively. The intensity of the band at ∼350 nm increases with decreasing pH. Addition of CH_3ONa to the acidified solution leads to a complete recovery of the "basic" spectrum, i.e., that of the free ligand, as ascertained from ^{1}H NMR spectroscopy (vide supra). From ^{1}H NMR data, it is clear that addition of CH_3ONa promotes rapid dissociation of the ligand from the metal center. However, the reversibility of the UV−vis spectral changes upon addition of HPF_6 indicates that the free vanadate remains available for complexation (cf. the corresponding ^{1}H and ^{51}V NMR spectra above). A weak broad absorption centered at ∼380 nm assigned as an LMCT band is observed under acidic conditions (see Figure 6). The absence of a significant absorption (i.e., LMCT bands) in the visible region of the spectrum and the similarity of the spectra of $\mathbf{1}^-$ and H_2L1 in methanol are in agreement with the spectroscopic features of related $[LV(=O)_2]$ systems.[1]

The electronic absorption spectrum of **2** in CH_3CN is shown in Figure 6, together with the changes in the UV−vis spectrum observed upon titration with HPF_6. Only minor changes in the absorption spectrum assigned to intraligand transitions ($\pi-\pi^*$) are observed (<450 nm) upon addition of HPF_6, whereas a red shift from 554 to 705 nm and a large increase in intensity of the visible absorption band are observed. The changes in the ligand-centered transitions (<450 nm) are complete upon addition of 1.1 equiv of HPF_6, whereas in contrast, a further increase in the intensity of the 705-nm band is observed up to 3 equiv of HPF_6. These results suggest that secondary processes occur, possibly involving protonation at two positions. As the first process involves protonation of the 1,2,4-triazole group, it is unlikely that the second step involves protonation of one of the V=O moieties, as two distinct species are observed in the ^{1}H NMR spectrum (vide supra). Hence, the steady increase in intensity observed is probably due to ligand-exchange processes (e.g., HO^- for CH_3O^-). Similar changes are observed in DMF, although addition of HPF_6 results in the appearance of a new absorption at 660 nm rather than 705 nm (vide infra, Figure 7). The low-energy absorption between 600 and 750 nm is assigned as an LMCT transition because of the increased intensity observed upon protonation. The decrease in the σ-donor strength of the 1,2,4-triazole upon protonation results in the metal center becoming more electron deficient and hence a better acceptor for the LMCT transition. Furthermore, the probability that it is the triazole unit that is protonated rather than the oxo ligands suggests that the transition is oxo-to-metal charge transfer.

Redox Properties of 1^- and 2. Complexes $\mathbf{1}^-$ and **2** exhibit redox behavior related to the presence of the phenolate ligands. For both complexes, anodic processes are observed between 1.0 and 2.0 V (vs SCE) that are irreversible and lead to electrode passivation after a single cycle (presumably because of phenol polymerization).[45] For complex $\mathbf{1}^-$, no metal- or ligand-localized redox processes were observed between 1.0 and −0.5 V, in neutral or acidic methanol/0.1 M KPF_6. In basic methanol solution and in CH_3CN/0.1 M TBAP, an anodic wave appears at 0.6 V, assigned to irreversible phenolate oxidation of the dissociated ligand $HL1^-$ (Figure S12). In DMF, irreversible reduction of vanadium(V) is observed at −1.26 V vs SCE at −40 °C (Figure S12).

For **2**, a well-defined V^{IV}/V^V redox couple is observed (Figure 8). In CH_3CN/0.1 M TBAP, a single reversible (ΔE_p = 70 mV, I_c/I_a = 1) reduction of the vanadium(V) center is found at 0.27 V ($E_{1/2}$). The very large positive shift in the oxidation potential compared to $\mathbf{1}^-$ reflects the increased electron density of the metal center from the methoxy ligand. Upon addition of 2 equiv of HPF_6 (based on the binuclear complex), a new quasireversible redox process at 0.63 V ($E_{1/2}$) is observed, together with a second reduction process at 0.37 V ($E_{p,a}$).[46] The anodic shift in the reduction potential under acidic conditions is, as expected, due to the reduction in electron density on the metal center upon protonation. When the water content of the HPF_6-acidified solution is

(45) (a) O'Brien, L.; Duati, M.; Rau, S.; Guckian, A. L.; Keyes, T. E.; O'Boyle, N. M.; Serr, A.; Görls, H.; Vos, J. G. *Dalton Trans.* **2004**, 514−522. (b) Paine, T. K.; Weyhermueller, T.; Bill, E.; Bothe, E.; Chaudhuri, P. *Eur. J. Inorg. Chem.* **2003**, *4*, 4299−4307.

(46) If 0.5 equiv of HPF_6 (based on a dinuclear complex) is added, then a superimposition of the protonated and deprotonated complexes is observed.

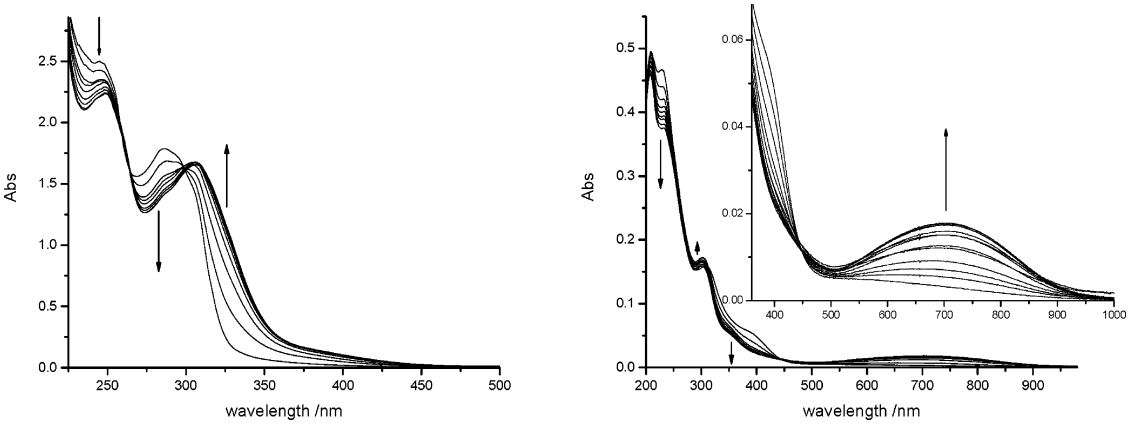

Figure 6. Electronic absorption spectra of (left) $\mathbf{1}^-$ in CH_3OH/CH_3ONa (2 equiv) with added HPF_6 (up to 10 equiv) and (right) titration of **2** with HPF_6 (until 4 equiv) in CH_3CN followed by UV−vis spectroscopy.

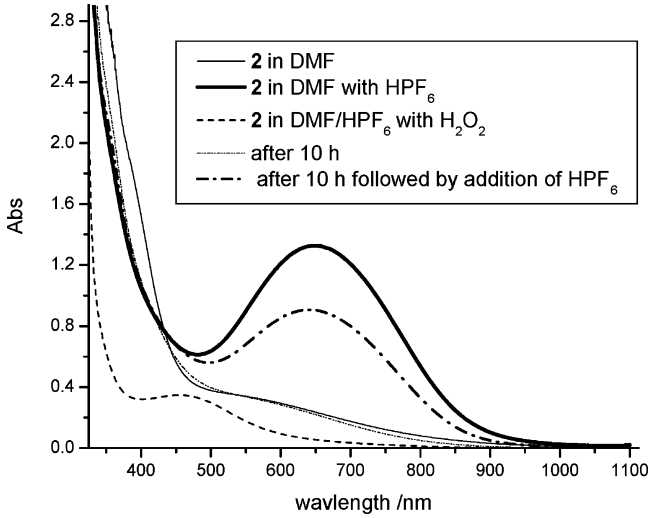

Figure 7. UV−vis absorption spectra of **2** in DMF with HPF_6 and H_2O_2.

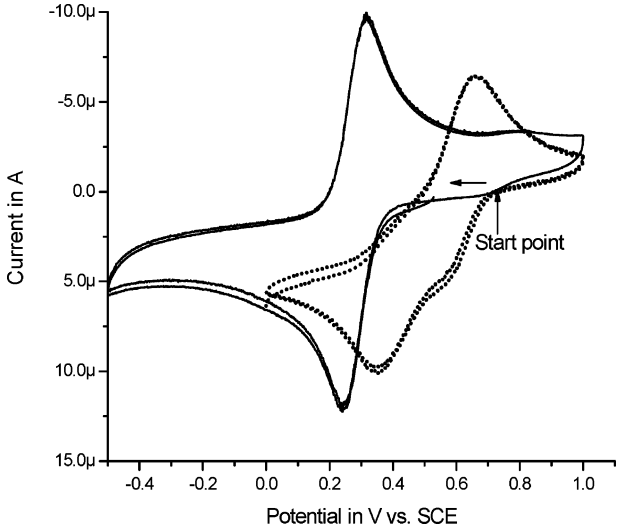

Figure 8. Cyclic voltammetry of **2** in CH_3CN (0.1 M TBAP) in the absence (solid line) and presence (dotted line) of (~2 equiv) HPF_6.

increased (or if $HClO_4$ is used instead of HPF_6), a marked change in the reversibility of the first reduction step takes place. Again, two reduction steps are observed by cyclic voltammetry at 0.63 and 0.37 V. Importantly, under thin-layer conditions at low scan rates (0.01 V s^{-1}), only the first, more positive cathodic wave (0.63 V) is observed, with the corresponding back-oxidation wave at $E_{p,a} = 1.2$ V. The absence of this wave in CH_3CN/HPF_6 is due to the slower exchange of CH_3O^- for H_2O/OH^- (indeed, under bulk electrolysis, the longer time scales allow for the 1.2 V process to become the dominant return wave). As the scan rate is increased to 5 V s^{-1}, the second process at 0.37 V becomes dominant, suggesting that this wave corresponds to the protonated form of **2** prior to ligand exchange (Figures S13 and S14). The 100 mV shift is in agreement with the shift in redox potentials observed for related Ru(II)-based systems.[40] This behavior suggests that the first cathodic process has its origin in a rapid (reversible) change to the coordination environment of the complex. The equilibrium is reached relatively slowly and, hence, it is more likely to be due to ligand exchange (e.g., CH_3CN/water) rather than protonation. Overall, the reduction and subsequent oxidation at 1.2 V do not result in dissociation of $L2^{3-}$, as confirmed by spectroelectrochemical studies (vide infra) and by reproducibility of the cyclic voltammogram before and after a controlled-potential bulk electrolytic reduction (at 0.3 V)/oxidation (1.2 V) cycle. Addition of base to this solution results in the reappearance of the single reversible cathodic process for complex **2**, albeit at a higher potential (0.3 V) than before the addition of acid.

In situ generation of the vanadium(IV) states of **2** in the absence and in the presence of HPF_6 was carried out in acetonitrile by both electrochemical and chemical reduction. Reduction of **2** at 0.275 V and subsequently at 0.0 V resulted in a decrease in absorption of the weak low-energy LMCT band at 554 nm together with the shoulder at 380 nm and in decreased intensity of the ligand-based absorption bands (Figures 9 and S15). The reduction at 0.275 V resulted in ~50% depletion compared to that at 0.0 V, indicating that a mixed-valence (V^VV^{IV}) species is not present and the reduction is of a mononuclear species, in agreement with NMR data (vide supra). Subsequent back-oxidation at 0.6 V leads to an almost complete recovery of the initial spectrum, confirming the stability of the complex in the V^{IV} state. For **2** under acidic conditions, a more complex situation is observed (Figure S16). Upon addition of HPF_6, a very intense absorption is observed at 705 nm that decreases in

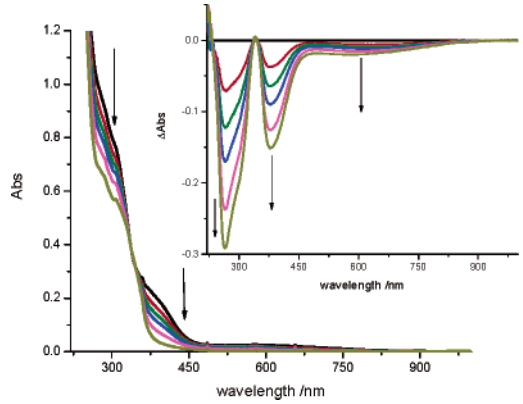

Figure 9. Spectroelectrochemistry of **2** in CH_3CN (0.1 M TBAP) at 0.0 V vs SCE. For full reduction/oxidation cycle, see Supporting Information Figure S15.

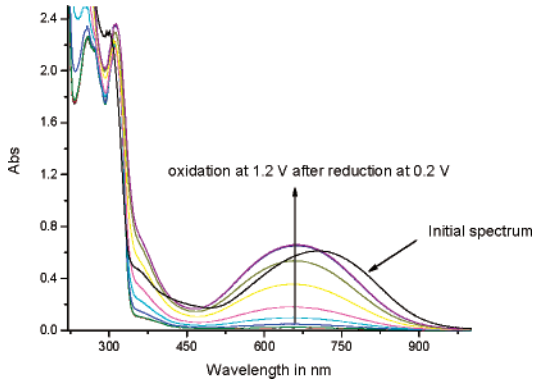

Figure 10. UV−vis spectroelectrochemistry of **2** in CH_3CN/HPF_6 followed by electronic spectroscopy. See also Supporting Information Figure S16.

intensity with time (in the presence of the platinum gauze electrode) and undergoes a hypsochromic shift to 680 nm. Reduction at 0.2 V accelerates this depletion, with a total bleaching of the visible absorption and a modification of the more intense (ligand-centered) UV bands. Subsequent oxidation at 1.2 V results in the reappearance of the visible absorption with similar intensity as observed for the initial spectrum, but with a pronounced blue shift in the absorption maximum to 660 nm (Figures 10 and S16). Subsequent reduction and oxidation cycles were fully reversible and showed no further change to the vanadium(IV) and vanadium(V) spectra, indicating that no further ligand-exchange reactions were occurring (and that, overall, the redox chemistry is chemically reversible). The pronounced initial blue shift of the visible absorption band is assigned to the ligand exchange of the methoxide ligand, based on the acid dependence for the ligand exchange and, more significantly, the blue shift of the absorption. It should be noted that the UV−vis spectrum after the reduction and subsequent reoxidation is very similar to that recorded for **2** in DMF/HPF_6, suggesting that the methoxide ligand is replaced by an aquo/aqua ligand rather than by acetonitrile.

Chemical reduction of both **2** and **2**/HPF_6 could be achieved using decamethylferrocene and ferrocene, respectively, as expected from the redox potentials of the deprotonated and protonated complexes. In each case, the UV−vis spectral changes were identical to those recorded in the course of the spectroelectrochemical experiments.

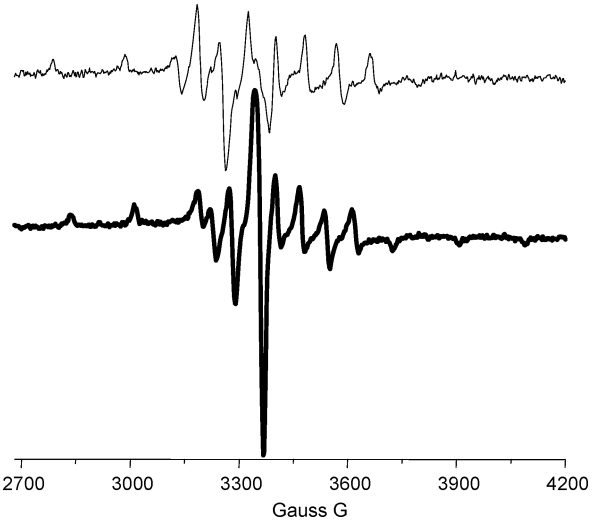

Figure 11. EPR spectra (77 K) of **2** (bottom) and H**2** (top) generated by electrochemical reduction at 0.0 and 0.4 V vs SCE, respectively, in CH_3CN (0.1 M KPF_6).

The effects of added perchloric acid (compared to protonation by HPF_6) or increased water content on the spectroelectrochemical response of **2**/HPF_6 are relatively minor, indicating that, at least for the vanadium(V) redox state, the same coordination mode is present as compared to protonation by HPF_6.

EPR Spectroscopy. Neither **1** nor **2** exhibits EPR signals at 77 K in different media (CH_3CN, DMF, or in methanol) as expected for the vanadium(V) oxidation state. Addition of HPF_6, CH_3ONa, or H_2O_2 does not yield an EPR-active species either, indicating that, under the conditions examined by NMR and UV−vis spectroscopies (vide supra), reduction of the vanadium center does not occur. Bulk electrolysis enabled the reversible generation of anisotropic EPR spectra of singly reduced **2** in the vanadium(IV) state (vide supra), which, at 77 K (in CH_3CN/0.1 M KPF_6), gave an EPR signal with well-resolved ^{51}V ($I = {}^7/_2$) hyperfine lines at $g_\perp = 1.927$ ($a_\perp = 161 \times 10^{-4}$ cm^{-1}) and $g_{||} = 1.983$ ($a_{||} = 56.9 \times 10^{-4}$ cm^{-1}) (Figure 11).[16c,47] The spectrum is typical of an octahedral coordination environment such as that found in imidazole-based complexes.[16c,48] Reduction in acidic solution (with HPF_6) or addition of acid to singly reduced $\mathbf{2}^-$ yields a considerably different EPR spectrum with $g_\perp = 1.933$ ($a_\perp = 182 \times 10^{-4}$ cm^{-1}) and $g_{||} = 1.876$ ($a_{||} = 67.2 \times 10^{-4}$ cm^{-1}) primarily because of an increase in $a_{||}$.

Interaction of $\mathbf{1}^-$ and 2 with H_2O_2. The solvent and pH dependence of the interaction of $\mathbf{1}^-$ and **2** with H_2O_2 was examined. In methanol under basic conditions, no interaction of $\mathbf{1}^-$ with H_2O_2 was established by ^1H NMR spectroscopy, as expected given the complete dissociation of $L1^{2-}$. However, in the absence of base, a very clear, reversible interaction with H_2O_2 is observed by both UV−vis and ^1H

(47) Plitt, P.; Pritzkow, H.; Oeser, T.; Kraemer R. *J. Inorg. Biochem.* **2005**, *99*, 1230−1237.
(48) Cornman, C. R.; Kampf, J.; Lah, M. S.; Pecoraro, V. L. *Inorg. Chem.* **1992**, *31*, 2035−2043.

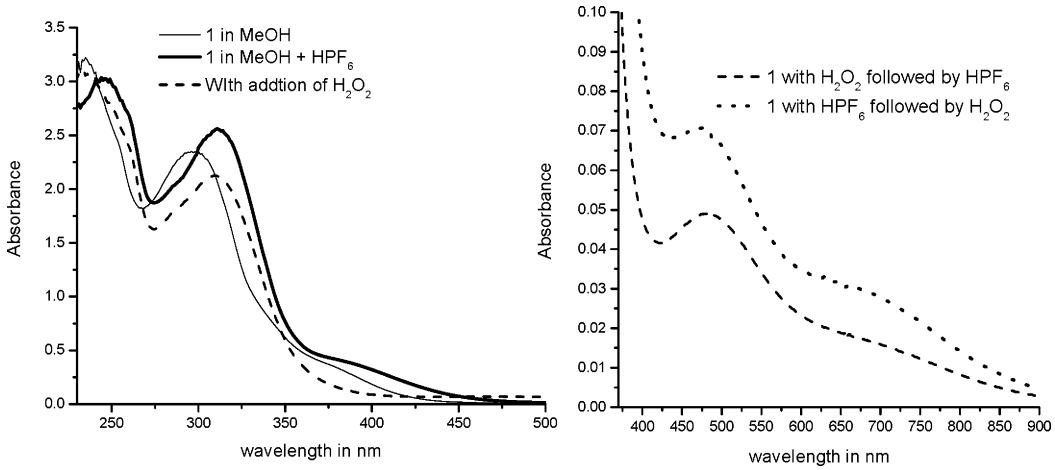

Figure 12. (Left) UV−vis spectra upon addition of HPF_6 followed by H_2O_2 to $\mathbf{1}^-$ in methanol. (Right) Effect of order of addition of HPF_6 and H_2O_2 on the UV−vis spectrum of $\mathbf{1}^-$ in methanol.

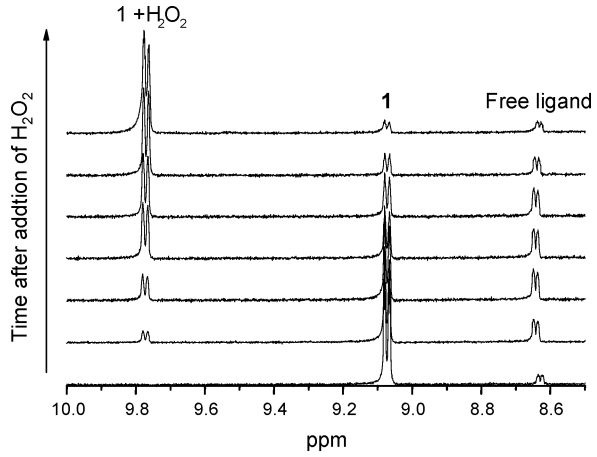

Figure 13. Evolution of the ^{1}H NMR spectrum of $\mathbf{1}^-$ in methanol upon addition of H_2O_2. The signal intensity is normalized to the solvent CD_2-HOD signal; spectra were recorded at 15-min intervals. For complete spectra, see Supporting Information Figure S18.

NMR spectroscopies with only limited ligand dissociation (Figures 12 and 13, respectively). The slow depletion of the spectrum of $\mathbf{1}^-$ is accompanied by the concomitant rise of a single new species upon addition of excess H_2O_2. The original spectrum (albeit with some free ligand present) is recovered eventually over a period of 2 days at 20 °C (Figures S17 and S18).

As described above, the effect of acid addition (HPF_6) on the UV−vis spectrum of $\mathbf{1}^-$ is pronounced, with a bathochromic shift and a modest increase in intensity of the lowest-energy absorption bands. Addition of H_2O_2 to the protonated complex causes a rapid hypsochromic shift of the main UV absorption band and the appearance of two low-intensity bands in the visible region. Similarly, addition of HPF_6 after addition of H_2O_2 yields an identical spectrum, indicating that the interaction with peroxide under neutral and acidic conditions yields the same "activated" complex. The presence of a pH dependence for the H_2O_2-activated complex (in both the UV−vis and ^{1}H NMR spectra) suggests that the ligand HL1 remains coordinated. Addition of H_2O_2 to a methanolic solution of **1** results in the appearance of a negative ion at *m*/*z* 335 ($\mathbf{1}^- + {}^{16}O$), assigned to $[L1VO_3]^-$ and a new signal at −567 ppm in the ^{51}V NMR spectrum. Under acidic conditions, a strong signal at *m*/*z* 337 assigned to $[HL1VO_2\text{-}OH]^+$ is observed in the presence of H_2O_2. Addition of H_2O_2 to **1**/HPF_6 results in the appearance of a new ^{51}V NMR signal at −515 ppm, with an absorption at −340 ppm assigned to interaction of the free vanadate with H_2O_2 (Figure S19).

In DMF, the stability of complex $\mathbf{1}^-$ is increased significantly compared to that in methanol, with no evidence for ligand dissociation. In contrast to methanol, addition of H_2O_2 does not lead to any change in the UV−vis or ^{1}H NMR spectrum. In the presence of HPF_6, however, a very rapid reaction with H_2O_2 is observed (Figures S5 and S20). As in methanol, a blue shift in the main ligand-centered absorption and the appearance of a weak absorption in the visible region are observed.

For **2** in CH_3CN, a clear and rapid reaction with H_2O_2 is observed as an initial depletion in the visible absorption bands and increase in the absorption at 315 nm, followed by a slower recovery of the visible absorption (over 200 s), albeit with distinct differences from the original spectrum (Figures S21 and S22). In the ^{51}V NMR spectrum, addition of H_2O_2 leads to the observation of additional absorptions between −150 and −550 ppm. However, the absorption at −505 ppm recovers with time (Figure S23). Addition of H_2O_2 results in the appearance of an additional peak in the ESI-MS spectrum at *m*/*z* 350 assigned, tentatively, to the complex $[V^V(L2^{3-})(OH)(OO)]^-$. For **2** in CH_3CN/TBAP in the presence of an excess of H_2O_2, the reduction process at 0.27 V becomes completely irreversible. Even at high scan rates, no depletion in the intensity of the cathodic wave was observed; however, the absence of a catalytic wave precludes the possibility of fast reoxidation to the vanadium(V) state by H_2O_2. The effect of H_2O under acidic conditions (vide supra), which results in reversible ligand exchange, suggests that the irreversibility is due to solvent ligand exchange rather than rapid reoxidation by H_2O_2. Under acidic conditions, addition of H_2O_2 leads to the formation of ammonium (1/1/1 triplet at ∼6.0 ppm) and several new absorptions in the aromatic region (eight resonances) of the ^{1}H NMR spectrum and two new absorptions at −556 and −718 ppm in the ^{51}V NMR spectrum (Figure S11).

Scheme 1. Tentative Structural Assignment for Species Observed for Complex $\mathbf{1}^-$ in Solution

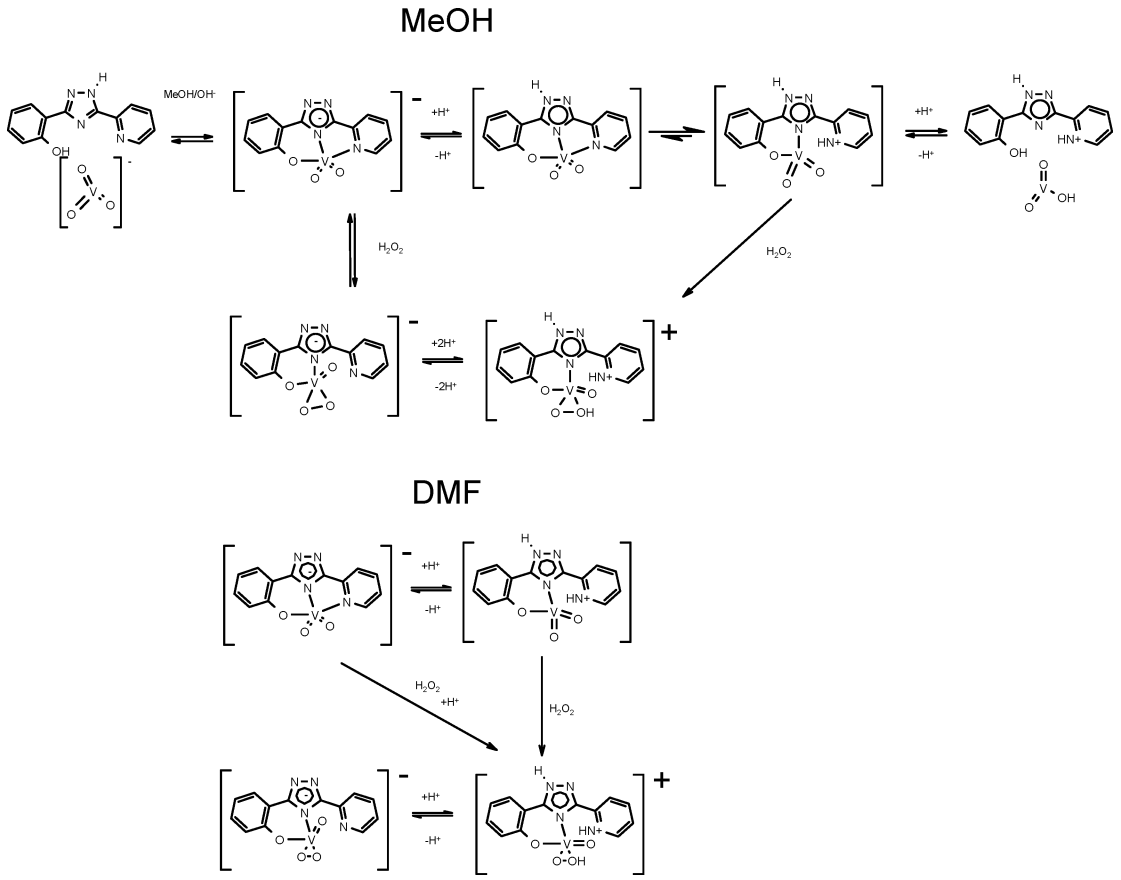

In DMF, addition of H_2O_2 to **2** results in very rapid changes in the UV−vis absorption spectrum and both the ^{1}H and ^{51}V NMR spectra. In time, a complete recovery of the initial spectrum of **2** is observed (Figures 4, 5, and S24). In the presence of HPF_6, addition of H_2O_2 to **2** leads to changes in the UV−vis spectrum similar to those observed for **2** in the absence of HPF_6. However, the spectrum recovers to that of **2**, and further addition of HPF_6 is required to reform the original protonated species (Figures 4, 5, and S25).

Summary

Schematic diagrams for the various pH- and H_2O_2-dependent processes observed for $\mathbf{1}^-$ and **2** in methanol and acetonitrile, respectively, and for both complexes in DMF are presented in Schemes 1 and 2.[49]

In DMF, complex $\mathbf{1}^-$ is stable toward ligand dissociation and undergoes a single protonation step. Surprisingly, the reaction with H_2O_2 requires addition of acid, presumably because of the requirement to labilize a V═O bond. In methanol solution, for $\mathbf{1}^-$, rapid pH-dependent ligand dissociation/association is observed. Whereas ligand dissociation occurs in basic solution, in the presence of acid, two vanadium species are observed by ^{1}H and ^{51}V NMR spectroscopy. In contrast to DMF, acid is not required to enable reaction with H_2O_2, and again, the reaction is reversible with time, and the peroxy species formed shows acid−base chemistry also. The similarity of the ^{1}H NMR spectra of $\mathbf{1}^-$ in methanol and DMF indicates that the molecular structure of $\mathbf{1}^-$ is retained upon dissolution in both solvents. In the presence of acid and/or H_2O_2, it is apparent that quite different species are formed in methanol than in DMF.

For complex **2**, no instability toward ligand ($L2^{3-}$) dissociation is observed; however, exchange of the methoxy units does occur, the rate of which is dependent on solvent, redox state, pH, and H_2O_2 addition. In acetonitrile, addition of acid leads to protonation of the 1,2,4-triazole unit and a partial exchange of the methoxide ligand.

In acetonitrile, reduction of **2** to the vanadium(IV) state is fully reversible; however, either addition of HPF_6 to **2** in the vanadium(IV) state or reduction of **2** in the presence of HPF_6 results in ligand exchange (most probably of the methoxide ligand with HO^-) to yield, in both situations, the same species. Oxidation of the reduced (protonated) complex **2** [vanadium(IV) state] is followed by deprotonation (because of the greater acidity of the high oxidation state). In DMF, ligand (methoxide) exchange occurs to a much greater extent than in acetonitrile both in the absence and in the presence of HPF_6. In contrast to acetonitrile, in DMF, addition of H_2O_2 in the absence of acid does not result in reaction with **2**. In acidic DMF, the reaction is fully reversible.

(49) The choice of solvents for the present study was governed, primarily, by the solubility of the complexes. In addition, the use of two different solvents for each complex allowed for the probing of solvent interactions, e.g., as ligands, and stability.

Scheme 2. Tentative Structural Assignment for Species Observed for Complex **2** in Acetonitrile and DMF Solution (S = Solvent)

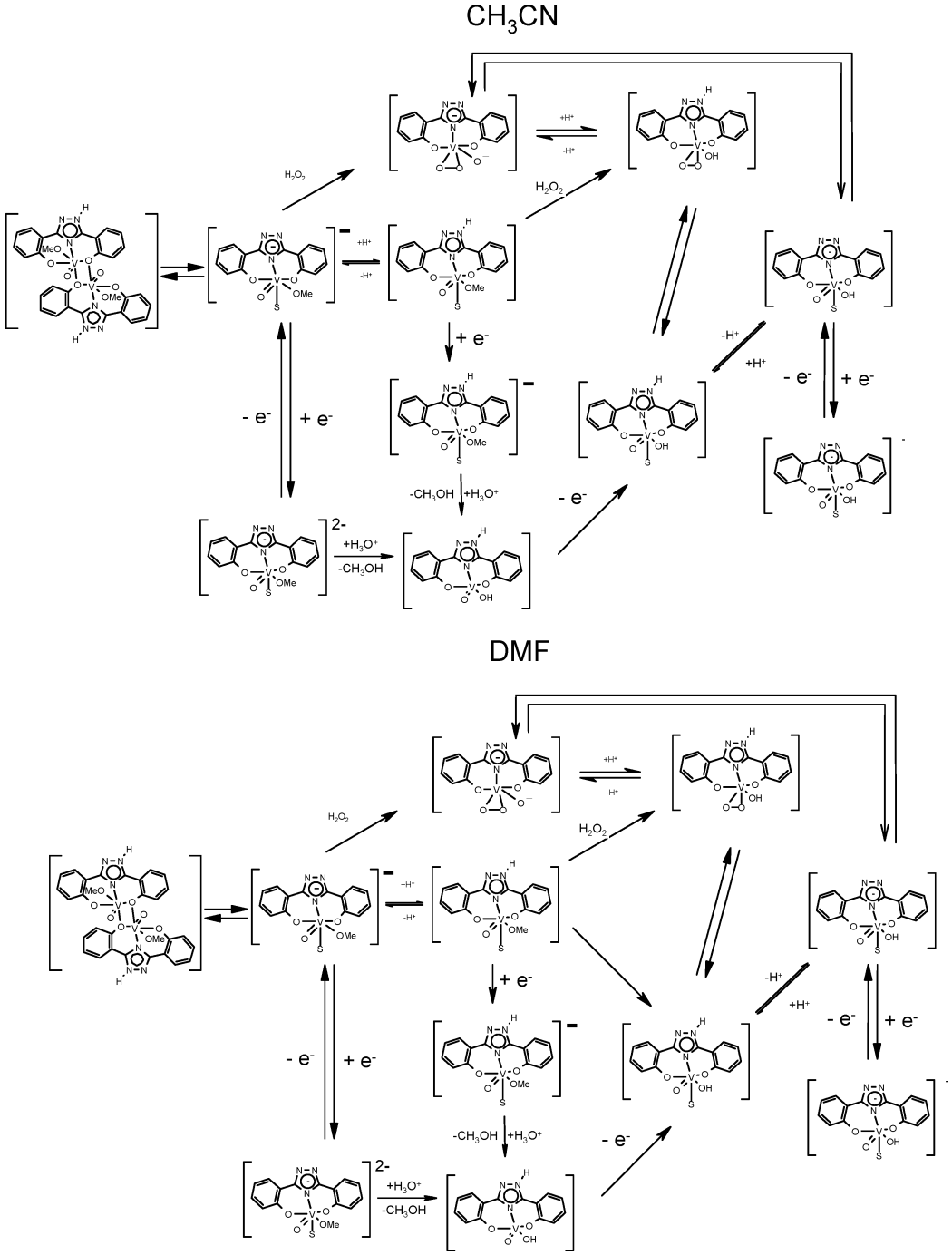

Conclusions

A difficulty encountered in the application of d^0 vanadium-based catalysts in oxidation chemistry is the propensity for these complexes to engage in rapid ligand-exchange reactions.[1] The interaction with hydrogen peroxide and the role of solvent in determining the stability of vanadium complexes was highlighted recently by Finke and co-workers in their study of a broad range of vanadium-based catechol dioxygenases.[11a] This inherent lability arises from the absence of crystal field stabilization for the vanadium(V) ion. Hence, in examining the activity of a vanadium(V) complex toward catalytic oxidation, it is essential to establish the integrity of the complex under catalytic conditions both prior to and after addition of H_2O_2.[11a] Although $\mathbf{1}^-$ and **2** exist, in the solid state, as mononuclear and binuclear complexes, respectively, it is apparent that, in solution, both complexes are essentially mononuclear. In the case of **2** in CH_3CN and DMF, the single ^{51}V NMR absorption that showed no temperature dependence confirms that, although association of two mononuclear complexes might occur, no significant change to the solvent coordination sphere or interaction between the metal centers is apparent.

The effect of H_2O_2 addition on complexes $\mathbf{1}^-$ and **2** shows considerable solvent dependence. A key finding for both complexes is that reaction with H_2O_2 is promoted under acidic conditions, which holds particular relevance for

oxidation catalysis. The catalytic properties of $\mathbf{1}^-$ and **2** were reported previously.[2b] Although significant changes occur for both $\mathbf{1}^-$ and **2** in the presence of H_2O_2, decomplexation of the ligands is not observed; indeed, well-defined metastable "H_2O_2-activated" complexes are observed. Hence, the catalytic activity[2b] is attributed to the complex and not vanadium(V) species uncoordinated to either H_2L1 or H_3L2. In addition, both electrochemical and EPR spectroscopic studies indicate that the complexes remain in the vanadium(V) oxidation state in the presence of H_2O_2.

For $\mathbf{1}^-$, two solvent-dependent processes should be noted. First, the stability of the complex toward dissociation of $L1^{2-}$ is dependent on both pH and solvent. Indeed, the better stability of $\mathbf{1}^-$ in DMF compared to methanol indicates that the presence of DMF under reaction conditions for catalytic oxidation would be favorable. However, the lack of interaction of $\mathbf{1}^-$ with H_2O_2 in DMF in the absence of HPF_6 might explain the lack of significant catalytic activity of $\mathbf{1}^-$ in earlier studies.[2b]

For **2**, similar pH and H_2O_2 dependence is observed in both CH_3CN and DMF. However, the dependence revealed by ^{1}H NMR, ^{51}V NMR, and UV−vis spectroscopies indicates that solvent coordination to the complex is an important process. Nevertheless, in both solvents, interaction with H_2O_2 does not result in decomposition of the complex, but especially in DMF, the importance of acid in the reaction with H_2O_2 is, again, apparent.

The introduction of the pH-sensitive 1,2,4-triazole unit into vanadium complexes has opened a new avenue to the tuning of the properties of these complexes. The effect is not limited to control of redox and electronic properties but includes also the interaction of these complexes with hydrogen peroxide. In addition, the nature of the solvent is critical in achieving interaction and, moreover, in stabilizing both vanadium complexes.

Acknowledgment. The authors thank Mrs. C. M. Jeronimus-Stratingh for performing the ESI-MS measurements and Mr. W. Kruizinga for assistance with ^{51}V NMR spectroscopic experiments. Prof. J. G. Vos and Prof J. Reedijk are thanked for helpful discussions and suggestions. This work was supported in part (M.L. and A.L.S.) by the Council for Chemical Sciences of The Netherlands Organization for Scientific Research (CW-NWO), The Netherlands Foundation for Chemical Research, Unilever R&D Vlaardingen (A.G.J.L., B.L.F., and R.H.), and the Dutch Economy, Ecology, Technology (EET) program, a joint program of the Ministry of Economic Affairs, the Ministry of Education, Culture and Science, and the Ministry of Housing, Spatial Planning and Environment (W.R.B., J.W.d.B., T.A.v.d.B., and B.L.F.).

Supporting Information Available: ^{1}H and ^{51}V NMR, UV−vis, and FTIR spectra of compounds $\mathbf{1}^-$ and **2**. This material is available free of charge via the Internet at http://pubs.acs.org.

IC051848X